2001

# Multifibre spectroscopy of the supernova remnant candidate RCW 114

Andrew Walker
*University of Wollongong*, ajw01@uow.edu.au

William Zealey
*University of Wollongong*, zealey@uow.edu.au

# Multifibre spectroscopy of the supernova remnant candidate RCW 114


## Abstract

RCW 114 is a filamentary nebula of about 250 arcmin diameter. Based on its large diameter-to-filament-width ratio, the expansion velocity, distance and size of the shell, it has been suggested that RCW 114 is a supernova remnant in its momentum-conserving phase. Confirmation of this identification is important, as the large angular size and extensive optical emission of this object will allow for detailed study to improve our knowledge of supernova remnants and their interaction with the interstellar medium.

We have used the FLAIR instrument on the UK Schmidt Telescope to obtain optical spectra of several filaments in RCW 114. These confirm that the emission is being produced by the interaction of the shock wave of a supernova remnant with the surrounding interstellar medium. We also obtained narrow-band H$\alpha$+[N ii] and [S ii] images to examine the spatial variation in ionization structure.



## Keywords

rcw, candidate, remnant, supernova, 114, multifibre, spectroscopy


## Disciplines

Engineering | Science and Technology Studies


## Publication Details

Walker, A. J. & Zealey, W. J. (2001). Multifibre spectroscopy of the supernova remnant candidate RCW 114. Monthly Notices of the Royal Astronomical Society, 325 (1), 287-292.

Mon. Not. R. Astron. Soc. **325,** 287–292 (2001)

# Multifibre spectroscopy of the supernova remnant candidate RCW 114

A. J. Walker★ and W. J. Zealey★
*Department of Engineering Physics, University of Wollongong, Northfields Avenue, Wollongong, NSW 2522, Australia*

Accepted 2001 February 14. Received 2001 February 9; in original form 2000 December 29

**ABSTRACT**

RCW 114 is a filamentary nebula of about 250 arcmin diameter. Based on its large diameter-to-filament-width ratio, the expansion velocity, distance and size of the shell, it has been suggested that RCW 114 is a supernova remnant in its momentum-conserving phase. Confirmation of this identification is important, as the large angular size and extensive optical emission of this object will allow for detailed study to improve our knowledge of supernova remnants and their interaction with the interstellar medium.

We have used the FLAIR instrument on the UK Schmidt Telescope to obtain optical spectra of several filaments in RCW 114. These confirm that the emission is being produced by the interaction of the shock wave of a supernova remnant with the surrounding interstellar medium. We also obtained narrow-band H$\alpha$+[N II] and [S II] images to examine the spatial variation in ionization structure.

**Key words:** surveys – ISM: bubbles – ISM: general – ISM: individual: RCW114 – supernova remnants.

## 1 INTRODUCTION

RCW 114 is a filamentary nebula of about 250 arcmin diameter located at RA (1950) = $17^h23^m$, Dec. (1950) = $-46°$. An H$\alpha$ exposure taken with the UK Schmidt Telescope shows the presence of filamentary emission around its full circumference, with less emission visible in the centre (Meaburn & Rovithis 1977). The presence of filaments down to 10 arcsec in width, along with an increase in the 29.9 MHz radio brightness in this region, led to their suggestion of this object being a supernova remnant (SNR).

Later work provided further evidence for this identification. Bedford et al. (1984) measured the interstellar Na I line at 5890 Å using the light of seven B stars coincident with and outside the nebula. These give RCW 114 a distance of $<200$ pc, a diameter of $<17.5$ pc, and an age of $\sim 2 \times 10^4$ yr.

Meaburn et al. (1991) obtained H$\alpha$ profiles in four positions. These show the nebula to be expanding at $V_{\rm exp} = 25$–$35\ {\rm km\ s^{-1}}$. In addition, their calculation of the kinetic energy of the shell, based on far-infrared flux densities from *IRAS* scans, gives a value consistent with that produced by a Type II supernova.

Presently RCW 114 is catalogued as a possible supernova remnant (Green 2000) with the identification G343.0–6.0. As discussed by Bedford et al. (1984), positive identification as a supernova remnant has not been possible, as a result of the non-detection of soft X-ray emission and the apparent absence of non-thermal radio emission. It has also been suggested that RCW 114 is associated with the Wolf–Rayet star HD 156385 (WR 90) (Cappa de Nicolau et al. 1988), however the star is far beyond RCW 114 at $\sim 2$ kpc (Bedford et al. 1984).

We have examined a 4850-MHz radio map of this area from the Parkes–MIT–NRAO survey (Griffith & Wright 1993). This clearly shows weak emission which strongly corresponds with the optical structure seen in H$\alpha$ emission. In addition, RCW 114 has also been identified at 2.4 GHz (Duncan et al. 1997), with the suggestion being made that it is a non-thermal source.

In light of this evidence, it seemed highly appropriate and timely that further study be made of this object. Here we present a spectroscopic study of RCW 114 conducted with the FLAIR instrument on the UK Schmidt Telescope. Our work is based on emission-line strengths and unambiguously shows that RCW 114 is a supernova remnant.

## 2 OBSERVATIONS AND REDUCTIONS

A 120-min exposure of RCW 114 centred on RA (1950) = $17^h20^m$, Dec. (1950) = $-46°$ was obtained in 1997 August with the UK Schmidt Telescope. This used the new H$\alpha$ filter (Parker & Bland-Hawthorn 1998) and Tech Pan film in order to record faint and fine details within the nebula.

The FLAIR fibre-optic system (Parker & Watson 1995) allows the observer to obtain spectra from up to 92 objects simultaneously within the telescope's field of $6° \times 6°$. This is ideal for this study because of the large angular size of the object, and because a large representative sample of the filaments of the object can be observed. In practice, when obtaining line ratios or fluxes for emission-line objects, less than half this number can be observed,

★E-mail: ajw01@uow.edu.au (AJW); zealey@uow.edu.au (WJZ)

**Table 1.** Details of FLAIR observations.

| Grating | Central wavelength (Å) | Wavelength range (Å) | Instrumental resolution (Å) | CCD resolution (Å pixel$^{-1}$) | Date | Frames |
|---|---|---|---|---|---|---|
| 600V | 6052 | 5288–6815 | 4.4 | 2.9 | 1997 Aug 28 | 4×1800 s |
| 600V | 4645 | 3926–5364 | 4.5 | 2.8 | 1997 Aug 29 | 3×1800 s |
| 300B | 5554 | 4070–7038 | 9.3 | 5.6 | 1997 Aug 29 | 3×1800 s |

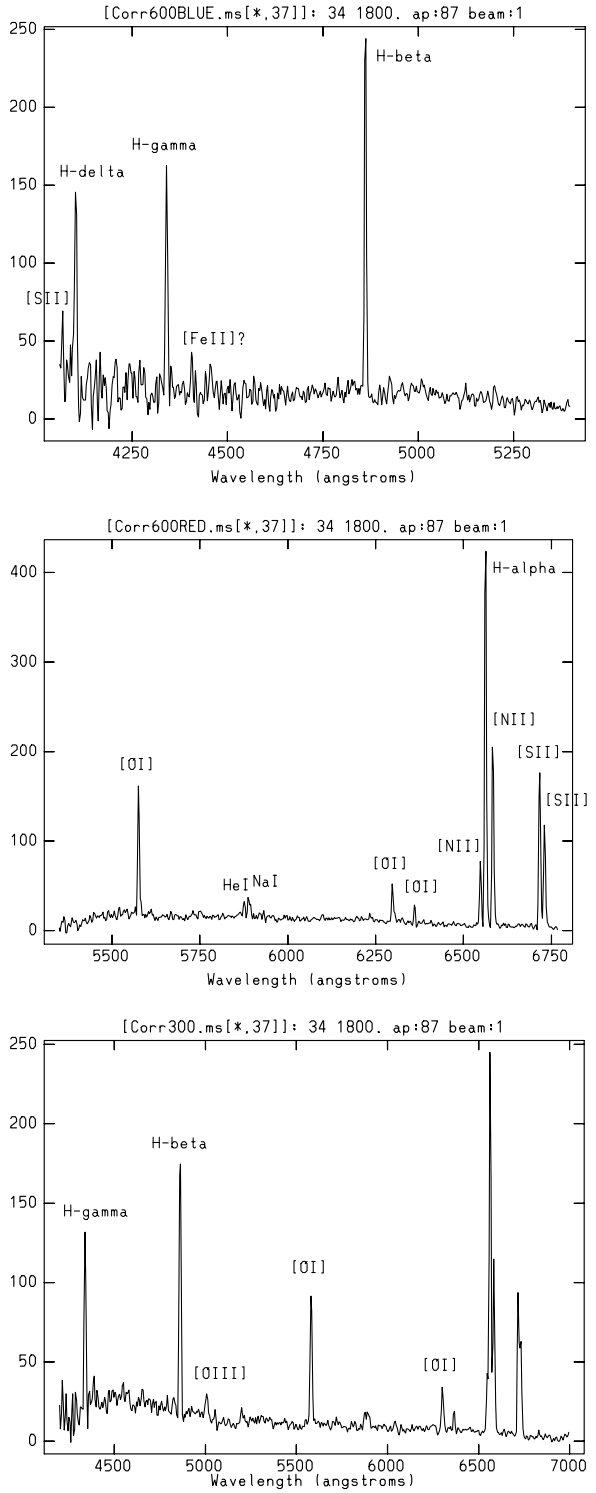


**Figure 1.** Three separate spectra of a bright filament in RCW 114. RA (1950) = $17^{h}31^{m}39^{s}$, Dec. (1950) = −45°46′.6 [S II]/H$\alpha$ = 0.69.

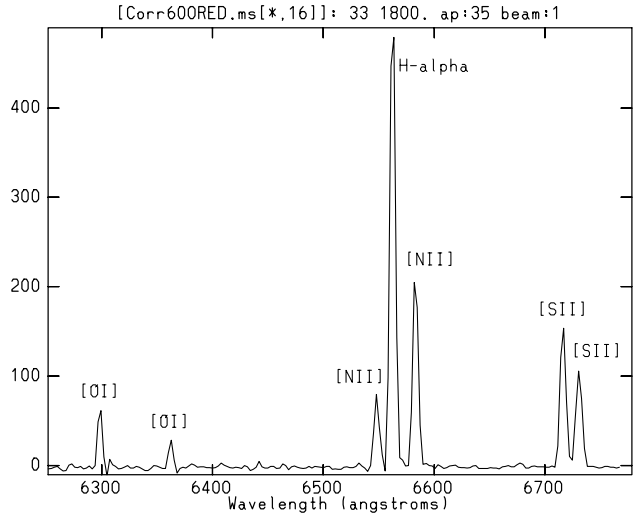


**Figure 2.** Enlarged red spectra of another filament at RA (1950) = $17^{h}30^{m}01^{s}$, Dec. (1950) = −46°11′.2. Here [S II]/H$\alpha$ = 0.55.

as a result of a small light leakage between adjacent fibres. A film copy of the RCW 114 H$\alpha$ image was made. This was used to select filaments to be observed. The film was attached to a metal backing-plate and the prism on the end of each fibre attached to the film in the position to be observed. This is then loaded into a plateholder for use in the telescope as described in Parker & Watson (1995).

Spectra were obtained at 34 object positions, other fibres were used for sky subtraction and image guiding on fiducial stars. The sky subtraction positions were chosen around the field in small regions free from stars with as little background emission as possible outside the main filamentary structure. Details of observations made are given in Table 1. For all observations the gratings were used 'blaze-to-camera'. In addition bias frames, arc frames and dome flats were obtained.

The data was reduced using the IRAF package, following a standard procedure developed for FLAIR data. The first main step is bias and flat correction using the CCDPROC procedure. The corrected frames for each observation are then combined. The DOFIBERS procedure is used to define apertures for each fibre spectra, which are traced along the dispersion axis. Dome flats are then used to correct for the efficiency of each fibre. Wavelength calibration is made using the arc frames. Corrected spectra are then extracted and sky-subtracted, using an average of the sky spectra. A correction for the wavelength response of the system was also made by comparing domeflats with blackbody curves calculated at the lamp temperature.

## 3 RESULTS

Representative spectra are shown in Figs 1 and 2. In the red, the spectra are dominated by the H$\alpha\lambda$6563, [N II] $\lambda\lambda$6548, 6583 and [S II] $\lambda\lambda$6717, 6731 lines. The close pairs are only partly resolved

with the 300B grating, but are clearly separated with the 600V grating. Emission from the [O I] and Na I lines is also visible: however, sky subtraction on these is generally poor, as seen on comparison of the high- and low-resolution spectra.

The blue end of the spectra is dominated by the H$\beta$, H$\gamma$ and H$\delta$ lines. In addition some spectra show evidence of weak emission from [O III] $\lambda\lambda$4949, 5007 and [Fe II], however these are for the most part not far above the noise level. Below 4250-Å wavelengths, many of the spectra are very noisy and show a sloped continuum, as a result of the low system response in this region. In addition the 100-$\mu$m width of the fibres led to stellar contamination in some spectra.

SPECFIT in IRAF was used to construct a model of the data in the wavelength range 6500–6750 Å. This consisted of a linear continuum background and Gaussian line profiles. Once a fit has been obtained to a desired accuracy level, it is possible to produce a list of fit parameters and errors calculated using the error spectra.

To estimate the error spectra, the following procedure was used. The square root was taken of each pixel of the combined data frame (before the IRAF DOFIBERS task was used). This was then divided by the square root of the number of frames, to estimate the error at each pixel. The result was processed with the DOFIBERS procedure in the same manner as the data frames, except that no sky subtraction was performed. From these error spectra, a table was produced for each separate set of spectra, listing the wavelength, flux value and estimated error of the flux at each data point.

To obtain more accurate line ratios, it was intended to correct line fluxes for interstellar reddening. This involves assuming an intrinsic H$\alpha$/H$\beta$ ratio of 3.0, and applying a correction based on the observed ratio. The observed ratio should be greater than 3.0, however in our response-corrected spectra the ratio was often much lower. This is likely to be a result of the lamp temperature being in error or the lamp deviating from a blackbody curve. As a result, no reddening corrections have been made. Our [S II]/H$\alpha$ results are still reliable, because of the small wavelength range involved and the proximity of RCW 114. Provided the reddening is not extreme, an examination of published results for this line ratio in SNR shows that ignoring reddening produces an error of only a few per cent in more reddened objects.

As a result of the position at which the sky spectra were taken, the subtracted spectra represent a combination of emission filaments and a more diffuse component from any extended nebulosity. The latter is below a few per cent of the intensity of the filamentary emission, and has only a small effect on the [S II]/H$\alpha$ ratios.

## 4 LINE DIAGNOSTICS

The most widely used supernova remnant diagnostic involving emission-line strengths is the [S II]$\lambda\lambda$6717, 6731/H$\alpha$ line ratio (Fesen, Blair & Kirshner 1985). When this ratio is observed to be greater than 0.5, it indicates the emission is being produced by shock-excited gas which has been swept up by a low-velocity shock. This can be compared with H II regions and planetary nebulae, where this ratio is usually much smaller, and H$\alpha$ is predominant. Unfortunately, the highest values of the ratio in these objects overlap the lowest values observed in SNR. In addition, [S II] emission may be very weak or absent in Balmer-dominated filaments [produced by high-velocity shocks travelling through an intercloud region, e.g. RCW 86 (Long & Blair 1990, Smith 1997) and the Cygnus Loop], and in oxygen-rich SNR (Weiler & Sramek 1988). Fesen et al. (1985) examine a number of other useful emission-line ratios, mainly involving oxygen and hydrogen lines.

In Table 2 we show the calculated line strengths for the five

**Table 2.** Observed emission-line strengths in RCW 114.

| Position (B1950.0) | | F($\lambda$) | | | | | Line ratios | | |
|---|---|---|---|---|---|---|---|---|---|
| R.A. | Dec. | [N II]$\lambda$6548 | H$\alpha\lambda$6563 | [N II]$\lambda$6583 | [S II]$\lambda$6717 | [S II]$\lambda$6731 | [S II]/H$\alpha$ | [N II]/H$\alpha$ | 6716/6731 |
| 17 11 16 | −46 13.9 | 17 ± 1 | 100 ± 1 | 55 ± 1 | 28 ± 1 | 18 ± 1 | 0.46 ± 0.01 | 0.72 ± 0.02 | 1.54 ± 0.08 |
| 17 11 19 | −45 52.6 | 13 ± 1 | 100 ± 1 | 44 ± 1 | 19 ± 1 | 13 ± 1 | 0.32 ± 0.01 | 0.57 ± 0.02 | 1.38 ± 0.11 |
| 17 12 29 | −45 14.3 | 15 ± 1 | 100 ± 1 | 44 ± 1 | 11 ± 1 | 9 ± 1 | 0.20 ± 0.01 | 0.58 ± 0.02 | 1.23 ± 0.16 |
| 17 13 34 | −46 25.1 | 15 ± 1 | 100 ± 2 | 50 ± 1 | 24 ± 1 | 18 ± 1 | 0.41 ± 0.01 | 0.66 ± 0.02 | 1.37 ± 0.09 |
| 17 13 49 | −44 56.4 | 14 ± 1 | 100 ± 1 | 47 ± 1 | 17 ± 1 | 12 ± 1 | 0.29 ± 0.01 | 0.61 ± 0.02 | 1.44 ± 0.12 |
| 17 14 31 | −44 55.7 | 17 ± 1 | 100 ± 1 | 51 ± 1 | 22 ± 1 | 15 ± 1 | 0.36 ± 0.01 | 0.68 ± 0.02 | 1.50 ± 0.09 |
| 17 15 22 | −46 06.9 | 18 ± 1 | 100 ± 1 | 53 ± 1 | 30 ± 1 | 19 ± 1 | 0.49 ± 0.01 | 0.71 ± 0.02 | 1.54 ± 0.07 |
| 17 15 25 | −46 48.3 | 15 ± 1 | 100 ± 1 | 47 ± 1 | 19 ± 1 | 13 ± 1 | 0.31 ± 0.01 | 0.62 ± 0.01 | 1.47 ± 0.07 |
| 17 16 34 | −46 04.3 | 15 ± 1 | 100 ± 2 | 51 ± 1 | 31 ± 1 | 21 ± 1 | 0.52 ± 0.02 | 0.67 ± 0.02 | 1.45 ± 0.09 |
| 17 16 42 | −47 13.1 | 16 ± 1 | 100 ± 1 | 54 ± 1 | 26 ± 1 | 19 ± 1 | 0.44 ± 0.01 | 0.71 ± 0.02 | 1.36 ± 0.08 |
| 17 16 52 | −45 31.9 | 17 ± 2 | 100 ± 3 | 59 ± 2 | 55 ± 2 | 39 ± 2 | 0.94 ± 0.04 | 0.75 ± 0.04 | 1.40 ± 0.08 |
| 17 18 57 | −47 25.0 | 15 ± 1 | 100 ± 2 | 48 ± 2 | 30 ± 1 | 22 ± 1 | 0.51 ± 0.02 | 0.63 ± 0.03 | 1.38 ± 0.10 |
| 17 19 14 | −46 38.6 | 14 ± 1 | 100 ± 2 | 50 ± 1 | 32 ± 1 | 22 ± 1 | 0.54 ± 0.02 | 0.64 ± 0.02 | 1.43 ± 0.07 |
| 17 19 40 | −47 00.4 | 15 ± 1 | 100 ± 2 | 47 ± 1 | 27 ± 1 | 19 ± 1 | 0.46 ± 0.02 | 0.62 ± 0.02 | 1.46 ± 0.09 |
| 17 20 17 | −47 46.8 | 15 ± 1 | 100 ± 2 | 57 ± 2 | 38 ± 2 | 24 ± 2 | 0.63 ± 0.03 | 0.72 ± 0.03 | 1.57 ± 0.12 |
| 17 22 18 | −45 39.2 | 21 ± 2 | 100 ± 3 | 59 ± 2 | 37 ± 2 | 22 ± 2 | 0.58 ± 0.03 | 0.80 ± 0.04 | 1.68 ± 0.16 |
| 17 22 23 | −46 17.8 | 19 ± 1 | 100 ± 2 | 58 ± 2 | 30 ± 1 | 20 ± 1 | 0.51 ± 0.02 | 0.77 ± 0.03 | 1.49 ± 0.12 |
| 17 22 46 | −47 37.8 | 11 ± 2 | 100 ± 3 | 43 ± 2 | 30 ± 2 | 23 ± 2 | 0.53 ± 0.03 | 0.54 ± 0.04 | 1.30 ± 0.14 |
| 17 22 53 | −43 40.1 | 14 ± 1 | 100 ± 1 | 48 ± 1 | 30 ± 1 | 22 ± 1 | 0.52 ± 0.02 | 0.62 ± 0.02 | 1.39 ± 0.07 |
| 17 23 03 | −46 53.0 | 16 ± 1 | 100 ± 1 | 49 ± 1 | 33 ± 1 | 22 ± 1 | 0.54 ± 0.01 | 0.66 ± 0.02 | 1.53 ± 0.07 |
| 17 23 48 | −48 12.3 | 10 ± 2 | 100 ± 3 | 43 ± 2 | 33 ± 2 | 21 ± 2 | 0.53 ± 0.03 | 0.54 ± 0.04 | 1.56 ± 0.17 |
| 17 25 29 | −46 08.5 | 16 ± 1 | 100 ± 2 | 49 ± 1 | 35 ± 1 | 24 ± 1 | 0.59 ± 0.02 | 0.65 ± 0.02 | 1.43 ± 0.08 |
| 17 25 52 | −46 39.2 | 14 ± 1 | 100 ± 1 | 43 ± 1 | 34 ± 1 | 24 ± 1 | 0.57 ± 0.01 | 0.57 ± 0.02 | 1.42 ± 0.06 |
| 17 27 10 | −47 26.4 | 29 ± 1 | 100 ± 2 | 102 ± 2 | 67 ± 2 | 49 ± 2 | 1.16 ± 0.03 | 1.30 ± 0.04 | 1.38 ± 0.06 |
| 17 27 33 | −47 47.0 | 12 ± 1 | 100 ± 2 | 42 ± 1 | 39 ± 1 | 29 ± 1 | 0.68 ± 0.02 | 0.53 ± 0.02 | 1.34 ± 0.07 |
| 17 29 13 | −46 32.7 | 15 ± 1 | 100 ± 1 | 44 ± 1 | 30 ± 1 | 20 ± 1 | 0.50 ± 0.01 | 0.59 ± 0.01 | 1.47 ± 0.05 |
| 17 30 01 | −46 11.2 | 15 ± 1 | 100 ± 1 | 42 ± 1 | 32 ± 1 | 23 ± 1 | 0.55 ± 0.01 | 0.57 ± 0.01 | 1.43 ± 0.05 |
| 17 31 39 | −45 46.6 | 15 ± 1 | 100 ± 2 | 48 ± 1 | 41 ± 1 | 28 ± 1 | 0.69 ± 0.02 | 0.63 ± 0.02 | 1.50 ± 0.07 |
| 17 32 51 | −46 48.2 | 19 ± 3 | 100 ± 4 | 59 ± 3 | 53 ± 3 | 42 ± 3 | 0.95 ± 0.05 | 0.78 ± 0.05 | 1.27 ± 0.11 |

major lines in the red spectrum, along with some derived ratios. The line strengths have been scaled to H$\alpha$ = 100. The errors were determined as discussed above. The filaments observed were seen to cover a wide range of values for the [S II]/H$\alpha$ ratio, from a minimum of 0.20 to a maximum of 1.17. About half of these ratios are in the range 0.5–0.7. While some of the weaker features will have large errors, a large ratio was also observed in some of the stronger-emitting filaments. This indicates that the emission seen in RCW 114 is predominately produced by shock excitation.

## 5 OPTICAL IMAGES

In order to further examine the ionization structure of RCW 114, narrow-band images were taken with Mike Bessell's wide field imaging equipment (Buxton, Bessell & Watson 1998) at Siding Spring Observatory during 1998. The images were obtained using a 400-mm f/4.5 Nikkor-Q lens and a 2K × 2K SITe thinned CCD. Each pixel is 12 arcsec in size, the full image covers 7° × 7° of sky. Four 10-min exposures were taken of RCW 114 with each of the filters H$\alpha$ 55 Å (6563 Å), [S II] 25 Å (6732 Å), [O III] 25 Å (5016 Å) and red continuum 55 Å (6676 Å). Each image was processed using standard IRAF tasks. After bias, flat-field and dark-frame corrections, images were aligned and then combined.

No structure was visible in the [O III] or red continuum images. The H$\alpha$ and [S II] images were continuum-subtracted and had a 3 × 3 median filter applied to remove most of the remaining stellar images. While the [S II] emission is weaker, there is very little difference in the visible structure in both bands.

## 6 SPATIAL VARIATION

In Figs 3 and 4 we have plotted the [S II]/H$\alpha$ and [N II]/H$\alpha$ ratios respectively at each of the fibre positions, using the H$\alpha$ image described in Section 5. The first of these appears to be larger along the bright eastern filament, and smaller for the south-western filaments. The three measured filaments to the north-west have ratios typical of H II regions, while the single northern ratio is strong. These values show that the expanding shock is interacting more strongly with the ISM away from the Galactic plane, which lies to the north-west. No such clear pattern is visible in Fig. 4.

Two positions in the south-east stand out for having unusually high values for both of these ratios. The first is at RA (1950) = $17^{h}32^{m}51^{s}$, Dec. (1950) = $-46°48'$ on a long, faint filament, and the second at RA (1950) = $17^{h}27^{m}10^{s}$, Dec. (1950) = $-47°26'$ on a very small but bright filament. It is likely that these are in some way related and lie in front of or behind the other emission in this area.

## 7 DISCUSSION

By comparison with spectra of known remnants (Fesen et al. 1985), it can be seen that our results are consistent with spectra of an evolved SNR. This is also suggested by the weak radio emission which appears to trace the optical structure. This can be contrasted to the younger Vela SNR, where the radio flux is stronger, [O III]

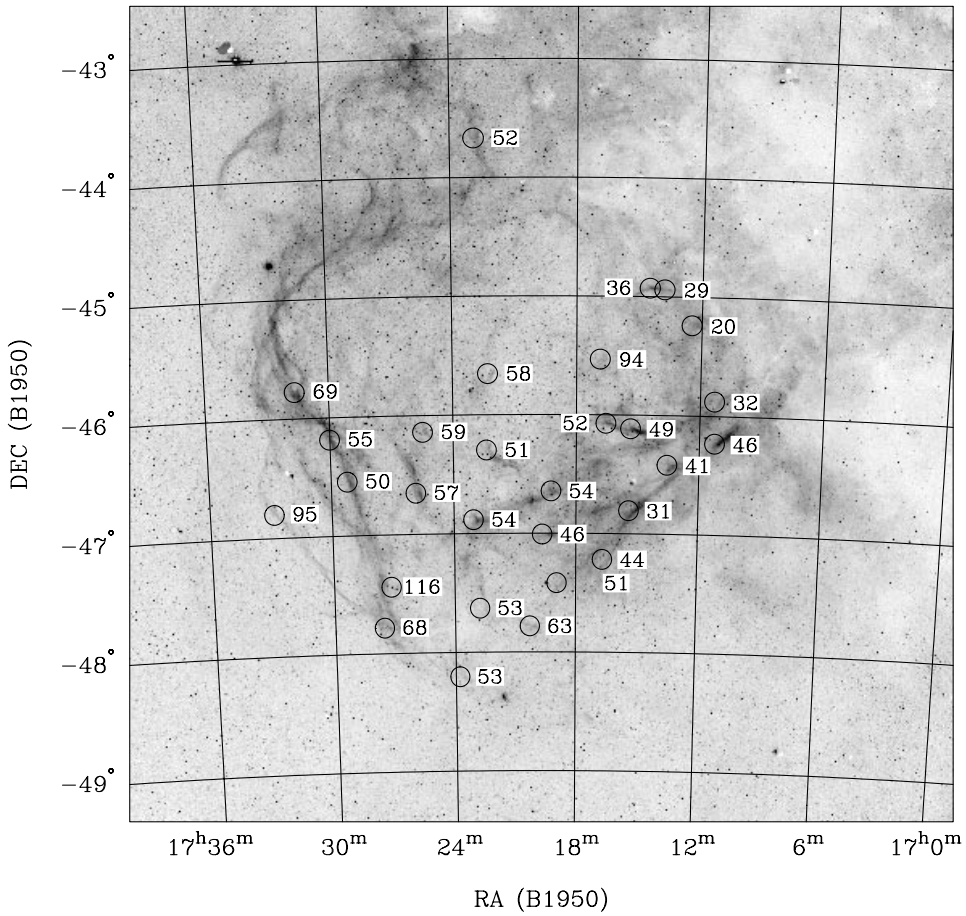


**Figure 3.** Plot of 100 × [S II]/H$\alpha$ for the observed positions in RCW 114.

emission is strong, and there is less correlation between optical and radio emission (Cram, Green & Bock 1998).

In Table 3 we present a list of all known large angular diameter (100 arcmin or more) SNR within the galaxy, including RCW 114. Of these RCW 114 is both the nearest and of the smallest physical size. As expected, the remnants with optical emission are generally closer. In contrast, despite being the closest, RCW 114 has weak radio emission. This, and its small physical size despite being well evolved, are suggestive of a weak initial explosion. This was also suggested by Bedford et al. (1984); however, their figure for the initial energy of $2 \times 10^{47}$ erg was later shown to be erroneous (Meaburn et al. 1991). Another possibility is that the remnant is

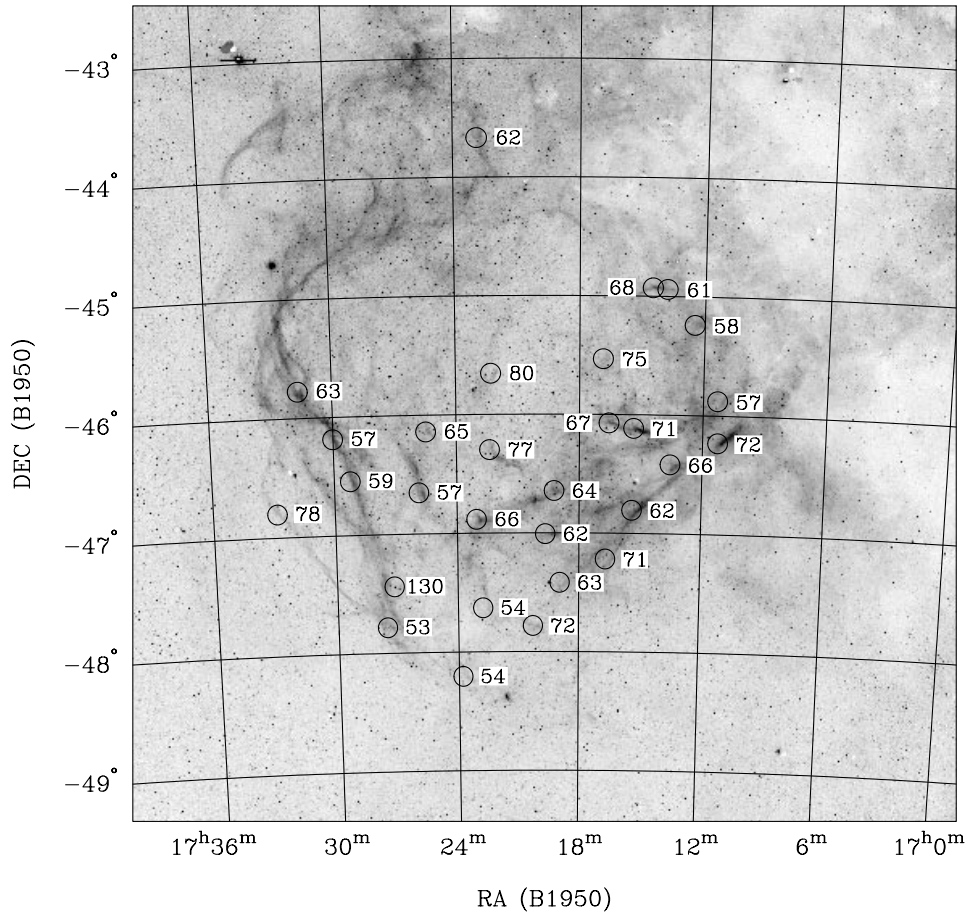


**Figure 4.** Plot of $100 \times$ [N II]/H$\alpha$ for the observed positions in RCW 114.

**Table 3.** Large angular diameter supernova remnants.

| Name | Diameter (arcmin) | Distance (kpc) | Distance Ref. | Diameter (pc) | Other names | Optical? |
|---|---|---|---|---|---|---|
| G 28.8+1.5 | 100 | <3.9 | 1 | <110 | | N |
| G 39.7−2.0 | 120×60 | 3.0 | 2 | 105×50 | W 50 | Y |
| G 65.3+5.7 | 310×240 | ~1 | 3 | 90×70 | | Y |
| G 74.0−8.5 | 230×160 | 0.8 | 4 | 54×37 | Cygnus Loop | Y |
| G 89.0+4.7 | 120×90 | 0.8 | 4 | 28×21 | HB 21 | Y |
| G 152.2−1.2 | 110 | 6.6 | 4 | 210 | | N |
| G 156.2+5.7 | 110 | 3.0 | 4 | 96 | | N |
| G 160.9+2.6 | 140×120 | 2.2 | 4 | 90×77 | HB 9 | Y |
| G 180.0−1.7 | 180 | 1.5 | 4 | 79 | S147 | Y |
| G 205.5+0.5 | 220 | 1.6 | 4 | 100 | Monoceros | Y |
| G 263.9−3.3 | 440 | 0.25 | 5 | 32 | Vela | Y |
| G 330.0+15.0 | 180 | 1.2 | 4 | 63 | Lupus Loop | Y |
| G 343.0−6.0 | 250 | <0.2 | 6 | <17.5 | RCW 114 | Y |

All diameter values are from Green (2000) except for Vela which is from Aschenbach (1993). Bonsignori-Facondi & Tomasi (1979) quote a distance for G 152.2–1.2 of 1.6 kpc.
References: 1 – Schwentker (1994); 2 – Dubner et al. (1998); 3 – Fesen, Gull & Ketelsen (1983); 4 – Case & Bhattacharya (1998) and references therein; 5 – Chan, Sembach & Danks (1999); 6 – Bedford et al. (1984).

expanding into a dense medium, and that after $\sim 2 \times 10^4$ yr the shock has diminished sufficiently so that radio emission is weaker and radiative cooling still significant.

The large angular size and extensive optical emission of RCW 114 will allow it to be studied in detail and greatly improve our knowledge of evolved SNR. In the future it will be important to obtain single-slit observations of some filaments, in order to confirm these results. Better sky subtraction will be possible, allowing us to obtain results on the oxygen lines and detect other fainter lines. These will be essential for a proper comparison with other evolved SNR.

We have also applied to obtain radio maps of small sections of RCW 114 using the Molonglo Observatory Synthesis Telescope (MOST), which has proved to be excellent in detecting extended non-thermal emission from SNR (Whiteoak & Green 1996). This will allow us to examine the relationship between H$\alpha$ and radio emission in both position and strength. It will also provide a second test of the SNR identification by comparison with *IRAS* data. In the longer term, an investigation of the radio continuum emission from RCW 114 will be useful. Links that can be established between observed properties in different wavelength regions will give a new insight into the processes and conditions within SNR.

## 8 CONCLUSIONS

We have shown that the optical emission being produced by RCW 114 is consistent with that expected of an evolved supernova remnant as suggested by earlier studies. This is confirmed by the weak radio emission and lack of detectable [O III] emission. A wide range of [S II]/H$\alpha$ ratios have been observed, suggesting that the interstellar medium into which it is expanding is non-uniform. This study has shown that the FLAIR fibre-optic system is very useful for the study of large and extended emission-line objects.

## ACKNOWLEDGMENTS

We would like to thank the staff of the UK Schmidt Telescope, especially Dr. Quentin Parker, for their help and advice in making these observations.

## REFERENCES

Aschenbach M., 1993, Adv. Space. Res., 131, 45
Bedford D. K., Elliot K. H., Ramsey B., Meaburn J., 1984, MNRAS, 210, 693
Bonsignori-Facondi S. R., Tomasi P., 1979, A&A, 77, 93
Buxton M., Bessell M., Watson B., 1998, PASA, 15, 24
Cappa de Nicolau C. E., Niemela V. S., Dubner G. M., Arnal E. M., 1988, AJ, 96, 1671
Case G. L., Bhattacharya D., 1998, ApJ, 504, 761
Chan A. N., Sembach K. R., Danks A. C., 1999, ApJ, 515, 25
Cram L. E., Green A. J., Bock D. C.-J., 1998, PASA, 15, 64
Dubner G. M., Holdaway M., Goss W. M., Mirabel I. F., 1998, AJ, 116, 1842
Duncan A. R., Stewart R. T., Haynes R. F., Jones K. L., 1997, MNRAS, 287, 722
Fesen R. A., Gull T. R., Ketelsen D. A., 1983, ApJS, 51, 337
Fesen R. A., Blair W. P., Kirshner R. P., 1985, ApJ, 292, 29
Green D. A., 2000, A Catalogue of Galactic Supernova Remnants (2000 August version). Mullard Radio Astronomy Observatory, Cambridge, UK (http://www.mrao.cam.ac.uk/surveys/snrs/)
Griffith M. R., Wright A. E., 1993, AJ, 105, 1666
Long K. S., Blair W. P., 1990, ApJ, 358, L13
Meaburn J., Rovithis P., 1977, Ap&SS, 46, L7
Meaburn J., Goudis C., Solomos N., Laspias V., 1991, A&A, 252, 291
Parker Q. A., Bland-Hawthorn J., 1998, PASA, 15, 33
Parker Q. A., Watson F. G., 1995, in Maddix S. J., Aragón-Salamanca A., eds, 35th Herstmonceux Conf., Wide Field Spectroscopy and the Distant Universe. World Scientific, Singapore, p. 33
Schwentker O., 1994, A&A, 286, L47
Smith R. C., 1997, AJ, 114, 2664
Weiler K. W., Sramek R. A., 1988, ARA&A, 26, 295
Whiteoak J. B. Z., Green A. J., 1996, A&AS, 118, 329

This paper has been typeset from a TEX/LATEX file prepared by the author.